

RESEARCH PAPER



USP38 inhibits colorectal cancer cell proliferation and migration via downregulating HMX3 ubiquitylation

Jun Wang[§], Yongxing Gu[§], Xueqin Yan, Jie Zhang, Jun Wang, and Yong Ding

Department of General Surgery, Huai'an People's Hospital of Hongze District, Huai 'An City, Jiangsu Province, China

ABSTRACT

Accumulating evidence has shown that H6 Family Homeobox 3 (HMX3) plays a crucial role in nervous system regulation. However, the regulatory mechanism of HMX3 in colorectal cancer (CRC) has seldom been studied. Herein, HMX3 was significantly downregulated in CRC, as demonstrated by qRT-PCR and WB analysis on clinical samples and a panel of cell lines. Besides, it was found that the expression of HMX3 was negatively correlated with survival of CRC patients. The functional analyses (EdU staining, CCK-8, colony formation, Transwell, and wound scratch assays) showed that CRC cell proliferation, migration, and invasion were significantly suppressed by HMX3 overexpression, while enhanced by HMX3 knockdown. Moreover, *in vivo* experiment revealed HMX3 overexpression could also suppress tumor growth. Combining bioinformatics and WB analysis, we preliminarily uncovered that HMX3 was involved in apoptosis and KRAS signaling pathways. Mechanistically, Ubiquitin-specific protease 38 (USP38) was identified as a novel post-translational regulator of HMX3, which could directly interact with HMX3 to stabilize its protein expression via deubiquitination. Furthermore, the role of USP38 silencing in promoting cell proliferation, migration, and invasion of CRC cells was blocked by HMX3 overexpression. In conclusion, our findings suggested that USP38/HMX3 axis is a novel promising therapeutic candidate for CRC.

ARTICLE HISTORY

Received 28 September 2021
Revised 10 December 2021
Accepted 4 January 2022

KEYWORDS

Colorectal cancer; deubiquitylating; H6 family homeobox 3; ubiquitin-specific protease 38; cell proliferation; migration; tumor growth

Introduction

Colorectal cancer (CRC) is a malignancy with a poor prognosis, and related to more than 900,000 deaths in 2020, which ranks the second in malignancy-related mortality globally and is the third common cancer globally [1]. Although CRC can be alleviated or cured by surgical resection, chemotherapy, radiotherapy, and other approaches, enormous patients fail to be cured and frequent recurrence contributes to poor survival [2]. Therefore, it is urgent to elucidate the underlying mechanism behind the tumorigenesis and progression of CRC to develop effective therapeutic strategy for CRC.


HMX3 (H6 family homeobox 3) is identified as a protein-coding gene, and diseases associated with HMX3 primarily include upper semicircular canal dehiscence and semicircular canal dehiscence syndrome [3]. In addition, as a transcription factor, HMX3 is involved in the regulation of nerve cell types, which is essential

for the development of the inner ear and hypothalamus [4–6]. However, up to date, the effect and molecular mechanism of HMX3 in cancer are hardly reported.

Post-translational modification (PTM) refers to the covalent and enzymatic modification of proteins after biosynthesis, including phosphorylation, acetylation, glycosylation, and ubiquitination [7]. As a protein modification method of PTM, ubiquitination has been implicated in the occurrence and progression of multiple cancers. Hence, people are increasingly interested in the therapeutic mechanism of the ubiquitination pathway in cancer. From a molecular point of view, ubiquitin is a small protein containing 76 amino acids that can bind to target proteins, thereby accelerating the degradation of target proteins [8]. It is noteworthy that ubiquitination processes are reversed by deubiquitylases (DUBs) [9], which regulate cellular processes and diseases, including cancer and

CONTACT Yong Ding ✉ winddr@sohu.com Department of General Surgery, Huai'an People's Hospital of Hongze District, 102 Dongfeng Road, Hongze District, Huai 'An City, Jiangsu Province 223100, China

[§]Jun Wang and Yongxing Gu are co-first authors.

 Supplemental data for this article can be accessed online at <https://doi.org/10.1080/15384101.2022.2042776>.

inflammation [10,11]. Recently, the critical role of DUBs in the development of cancer has been extensively demonstrated. It has been shown that cylindromatosis (CYLD) inhibited cell proliferation and tumorigenesis through deubiquitylating p18 [12].

As the biggest family of DUBs, Ubiquitin-specific proteases (USPs) can interact with different cellular targets to regulate numerous cellular functions, which have been reported to play important roles in development and progression of various types of cancer [13]. USP29 enhanced chemotherapy-induced stemness in non-small cell lung cancer through stabilizing Snail1 in response to oxidative stress [14]. USP8 enhanced tumorigenesis in breast cancer via deubiquitylating and stabilizing the intracellular domain of Notch1 [15]. USP38 also belongs to USPs family but research on its functions is limited. Recent studies on USP38 were mainly focused on its role in inflammation [16,17]. A recent study demonstrated that USP38 played a tumor suppressor role in CRC through suppressing chemoresistance and stemness of CRC cells [18]. Nonetheless, the role of USP38-mediated deubiquitination in the progression of CRC remains elusive.

In the present study, we examined the expression level of HMX3 in CRC tissues and cell lines, and analyzed the correlation between HMX3 expression with prognosis of CRC patients. Moreover, the effect of HMX3 on CRC cell proliferation, migration and invasion and the correlation between USP38 and HMX3 were explored. Finally, rescue experiment was performed to verify whether the interaction of USP38 and HMX3 is involved in cell proliferation, migration, and invasion in CRC. In summary, our study reveals a novel mechanism of USP38/HMX3 axis in CRC cell progression, which may be considered as a potential therapeutic target for CRC.

Materials and methods

Tissue collection

The principles of the World Medical Association Declaration of Helsinki were followed, and the protocol was approved by the Huai'an People's Hospital of Hongze District Ethics Committee.

All participants signed written informed consent before participating in the study. CRC tissues were obtained from 104 patients who received surgery in Huai'an People's Hospital of Hongze District from June 2005 to July 2010. Meanwhile, the corresponding adjacent normal CRC tissues were harvested from eight patients. None of the patients receive any treatment before surgery. Each patient was returned for follow-up visit with an interval of 3 months. Overall survival was defined as the date of operation to the date of death or the last contact. The tissue samples were immediately frozen in liquid nitrogen and stored at -80°C for the subsequent analysis of HMX3 expression at mRNA and protein levels.

Cell culture and transfection

Human CRC cell lines (HT29, HCT116, SW480, and LOVO cells) and human normal intestinal epithelial HIEC-6 cells were obtained from the American Type Culture Collection (ATCC, VA, USA), and were cultured in DMEM medium containing 10% FBS (Thermo Fisher Scientific, CA, USA) in a humidified incubator at 37°C with 5% CO_2 . The overexpression vectors of HMX3 (pcDNA-HMX3), USP38 (pcDNA-USP38) and corresponding control vectors (pcDNA-vector) were purchased from Fenghui Biotechnology Corporation (Changsha, China). shRNAs against HMX3 and USP38 were designed by Enjing Biotechnology Corporation (Nanjing, China) (supplementary Table S1). HCT116 and SW480 cells were transfected with indicated plasmids according to the instructions of lipofectamine 2000 (11,668-019; Invitrogen, CA, USA) and incubated for 48 h, which were then proceeded for subsequent experiments.

Tumor xenograft experiment

BALB/c athymic male nude mice (4–5 weeks old, 20 g) from Huai'an People's Hospital of Hongze District were used to construct xenograft mouse models. These animals were raised in a specific-pathogen-free (SPF) environment. HCT116 cells (1×10^6) with overexpressed HMX3 were injected subcutaneously into the flanks of nude mice. The tumor size was measured using a vernier caliper

every 4 days. The xenograft volumes were calculated using the formula $(L \times W^2)/2$. The mice were euthanized by cervical dislocation after feeding for 28 days, and the xenografts were dissected and weighed. All experiments were approved by the Animal Care and Use Committee of Huai'an People's Hospital of Hongze District. Animal welfare and experimental procedures were performed in accordance with the Guide for the Care and Use of Laboratory Animals.

Immunohistochemistry (IHC)

Three pairs of CRC cancerous and the adjacent normal tissues were fixed with 10% neutral formalin and embedded in paraffin, and 4- μ m thick sections were prepared. In summary, immunohistochemistry staining was performed as follows. The thick sections were deparaffinized and hydrated, followed by soaking in 3% H_2O_2 for 20 min at room temperature, and then subsequently incubated with anti-HMX3 (PA5-69,500, rabbit polyclonal antibody, Invitrogen, US) antibodies at 4°C overnight. The next day, the primary antibody was discarded, and the sections were washed with PBS for 5 min (three times). Then, the sections were washed with PBS for 5 min (three times) after the addition of secondary antibody (1:200, SignalStain® Boost IHC Detection Reagent, CST, USA) for 50 min. Finally, freshly prepared diaminobenzidine (DAB) was added for color development, and the sections were counterstained with hematoxylin (Solarbio, China), dehydrated, and mounted with neutral gum. All slides were observed and photographed under a microscope ($\times 200$ and $\times 400$). The expression levels of target proteins in tissues were determined by two independent pathologists blinded to the clinical characteristics of the patients according to the determination of cell staining proportion and intensity.

Cell counting kit-8 (CCK-8)

The HCT116 and SW480 cells with a density of 2×10^3 cells per well and 150 μ L of a freshly prepared preheated mixture were added into a 96-well plate with a solution containing 10% CCK-8 (Sigma, USA). At the same time, a blank control

well containing the mixture of α -MEM and CCK-8 was set, and the plate was incubated at 37°C for 1 h. The optical density (OD) value was determined at 450 nm using a spectrophotometer at 24, 48 and 72 h, respectively.

Colony formation assay

As a gold standard to determine cell reproductive death after treatment, colony formation assay was used to detect “unlimited” division of every cell in the population [19]. The assay was carried out as per the protocol proposed by Brix, et al. [20]. In brief, HCT116 and SW480 cells were seeded into 6-well culture plates at a density of 1×10^3 cells per well, and incubated with 37°C and 5% CO_2 for 2 weeks. At the indicated time points, the culture medium was removed, and cells were briefly rinsed with PBS. Then, the formed colonies were fixed with 4% paraformaldehyde for 20 min and stained with 1% crystal violet (Sigma-Aldrich) for 30 min, and stained colonies were counted under an inverted microscope.

Ethylenediurea (EdU) staining assay

Briefly, HCT116 and SW480 cells were cultured in 96-well plates at 5×10^3 cells per well for 48 h incubation. Then, 100 μ L of complete medium containing 0.2 μ L of EdU working solution was added to each well (CWBiotech, Beijing, China) for another 3 h cultivation. After that, they were fixed in 4% paraformaldehyde and 50 μ L of glycine for 15 min and 5 min, respectively, and washed twice with 3% BSA. To permeabilize the cell membrane, the cells were incubated in 0.5% Triton X-100 for 20 min and washed twice with 3% BSA. According to the manufacturer instructions, the prepared mixture was added for 30 min, and the cells were washed twice with 3% BSA and once with PBS. The cells were finally incubated in the dark for 15 min and washed twice with PBS. DAPI was used to stain cell nuclei. The percentage of EdU-positive cells was calculated from five random fields in three wells under an inverted fluorescence microscope in a darkroom.

Transwell assay

To detect cell invasion, the indicated cells (3×10^5 cells/mL) were mixed with 100 μ L serum-free DMEM and seeded into an 8- μ m pore polycarbonate membrane with pre-coated Matrigel in the upper chamber according to the manufacturer's instructions (Corning Incorporated; NY, USA). In addition, the bottom chamber was filled with 600 μ L DMEM containing 10% FBS. After 48 h incubation, the invasive cells were fixed with 4% paraformaldehyde for 20 min at room temperature, and subsequently stained with 1% crystal violet for 30 min. Finally, cells in ten randomly selected views were counted.

Wound scratch assay

HCT116 and SW480 cells were seeded in a 6-well plate at a density of 10^3 cells per well and cultured in a 5% CO₂, 37°C constant temperature incubator for 24 h. The monolayers were scratched by a sterile pipette tip and then incubated for another 48 h. The cells were photographed by a microscope and the migration percentage was analyzed using ImageJ software (National Institutes of Health, MD, USA).

Western blotting (WB)

Tissues and cells (72 h after transfection) were washed once with iced PBS, and pH 7.4 RIPA buffer (1% Triton X-100, 10 mM Tris, 1 mM EDTA, 1 mM EGTA, 150 mM NaCl) and protease inhibitor mixture (1:100) were used to homogenize the tissues and cells. They were then centrifuged at 4°C. BioRad Bradford protein assay kit was used to measure protein concentration, and conduct protein electrophoresis SDS-PAGE. The protein was transferred to PVDF membranes and incubated with TBST (25 mmol/L Tris, pH 7.5, 150 mmol/L NaCl and 0.1% Tween 20) containing 5% bovine serum albumin for 1 h. The PVDF membrane was then incubated with antibodies at 4°C overnight. After washed three times with TBST, the membrane was reacted with the horseradish peroxidase-labeled secondary antibody for 1 h. Finally, enhanced chemiluminescence (ThermoFisher

Scientific, CA, USA) was used for color reaction, and imaging was performed using a chemi-Scope mini imaging system (Clinux Science, Shanghai, China). To analyze the results, band intensity was quantified by ImageJ software. The information of antibodies included in this study is listed in supplementary Table S2.

Co-immunoprecipitation (Co-IP) assay

The total protein of HEK 293 T cells with different transfections was extracted in Co-IP lysis buffer (Beyotime, Beijing, China). For immunoprecipitation (10001D, Invitrogen, CA, USA), the cell lysate was incubated with anti-flag (ab1162, Abcam) or anti-HA (3724, Cell Signaling) antibody and Dynabeads Protein G at 4°C overnight. Then, the beads were washed three times with lysis buffer, and the immunoprecipitates were collected for Western blotting analysis.

Deubiquitination assay

The indicated plasmids were transiently transfected into the HEK 293 T cells and maintained for 48 h. Then the cells were harvested and lysed in denatured lysis buffer after incubated with 10 μ M MG132 (Selleck) for 6 h. Anti-Flag M2 affinity gel (A2220, Sigma Aldrich) was used to immunoprecipitate HA ubiquitinated Flag-HMX3 and the Flag-HMX3 protein was purified and immunoblotted with anti-HA antibody (5017, Cell Signaling). Under denaturing conditions, endogenous HMX3 was immunoprecipitated with anti-HMX3 antibody (PA5-69,500, rabbit polyclonal antibody, Invitrogen, US). Finally, the endogenous HMX3 protein was purified and collected for immunoblotting with anti-ubiquitin antibodies (3936, Cell Signaling).

Half-life assay

To detect protein stability, the transfected cells were mixed with cycloheximide (CHX; 50 mg/mL) and incubated for 0, 2, 4, 6 h, respectively. Then, the post-incubation cells were collected and lysed, and the lysates were finally separated by SDS-PAGE for WB analysis of protein levels at each time point.

qRT-PCR

The qRT-PCR was performed to measure the expression of HMX3 mRNA. In brief, total RNA was extracted from CRC tissues and cells using a PureLink RNA Mini assay kit (Thermo Fisher Scientific, CA, USA). Then, the PrimeScript RT Reagent assay kit (Thermo Fisher Scientific, CA, USA) was used for the reverse transcription of RNA into cDNA. The Real-time PCR System and SYBR-Green PCR Master Mix (Applied Biosystems, CA, USA) were used to quantitatively determine mRNA levels. The PCR cycling conditions: initial denaturation at 95°C for 5 min, followed by 40 cycles at 95°C for 30 sec and 60°C for 30 sec. For this experiment, GAPDH was used as an internal reference and the formula $2^{-\Delta\Delta Ct}$ method was adopted to calculate the relative expression of the HMX3. $\Delta\Delta Ct = (Ct \text{ target gene} - Ct \text{ reference gene}) \text{ experimental group} - (Ct \text{ target gene} - Ct \text{ reference gene}) \text{ control group}$. All the reactions were performed in triplicate. The primer sequences (supplementary Table S3) were synthesized by Sangon Biotech (Shanghai, China).

Bioinformatics analyses

The expression profile of HMX3 and USP38 between CRC and normal tissues was analyzed based on ENCORI online database (<http://starbase.sysu.edu.cn/>).

The potential interacted genes of HXM3 were predicted using two bioinformatics tools, including BioGRID (<https://thebiogrid.org/>) and GeneMANIA (<http://genemania.org/>).

Gene Set Enrichment Analysis (GSEA) was applied to explore the potential pathways associated with the expression of HMX3 based on the CRC dataset downloaded from the TCGA database.

Statistical analysis

Statistical analysis was performed using SPSS 20.0 (Chicago, USA) software. The Student's t-test and one-way analysis of variance (ANOVA) were used to evaluate differences between two or multiple groups. Chi-square test or Fisher's exact test was used for comparisons between HMX3 expression

and clinical features. The Kaplan-Meier method was used to estimate overall survival. Measurement data were expressed as mean \pm standard error of the mean (SEM). $P < 0.05$ was considered statistically significant. Figures were generated with GraphPad Prism 7 (GraphPad Software, USA) and Adobe Illustrator CS6 (Adobe, USA).

Results

HMX3 is lowly expressed in CRC tissues and cell lines

To explore the correlation between HMX3 and CRC, the expression level of HMX3 in CRC and corresponding adjacent normal tissues was determined using WB, qRT-PCR, and IHC assays. The expression level of HMX3 in CRC tissues was significantly lower than that in adjacent normal tissues (Figure 1a-c), which was consistent with the data of ENCORI (Figure 1d). In addition, HMX3 was lowly expressed in CRC cell lines (HT29, HCT116, SW480, and LOVO), compared with human normal intestinal epithelial cells (HIEC-6) (Figure 1e). Additionally, the 104 CRC patients were classified into two groups according to the median ratio of HXM3 mRNA expression: high HXM3 mRNA expression group ($n = 47$) and low HXM3 mRNA expression group ($n = 57$). Kaplan-Meier survival curve demonstrated that CRC patients with low HMX3 expression exhibited poor overall survival than those with high HMX3 expression ($P < 0.05$, HR = 0.38, Figure 1f). Collectively, these data suggested that HMX3 was lowly expressed in CRC tissues and the low expression of HMX3 was associated with poor CRC prognosis, implying that HMX3 may function as a tumor suppressor gene in CRC progression.

HMX3 inhibits CRC cell proliferation in vitro and tumor growth in vivo

To assess the effect of HMX3 on the proliferation of CRC cells, HMX3 was overexpressed in CRC cells. WB and qRT-PCR analyses demonstrated that the HMX3 overexpression vector successfully up-regulated HMX3 expression at both mRNA

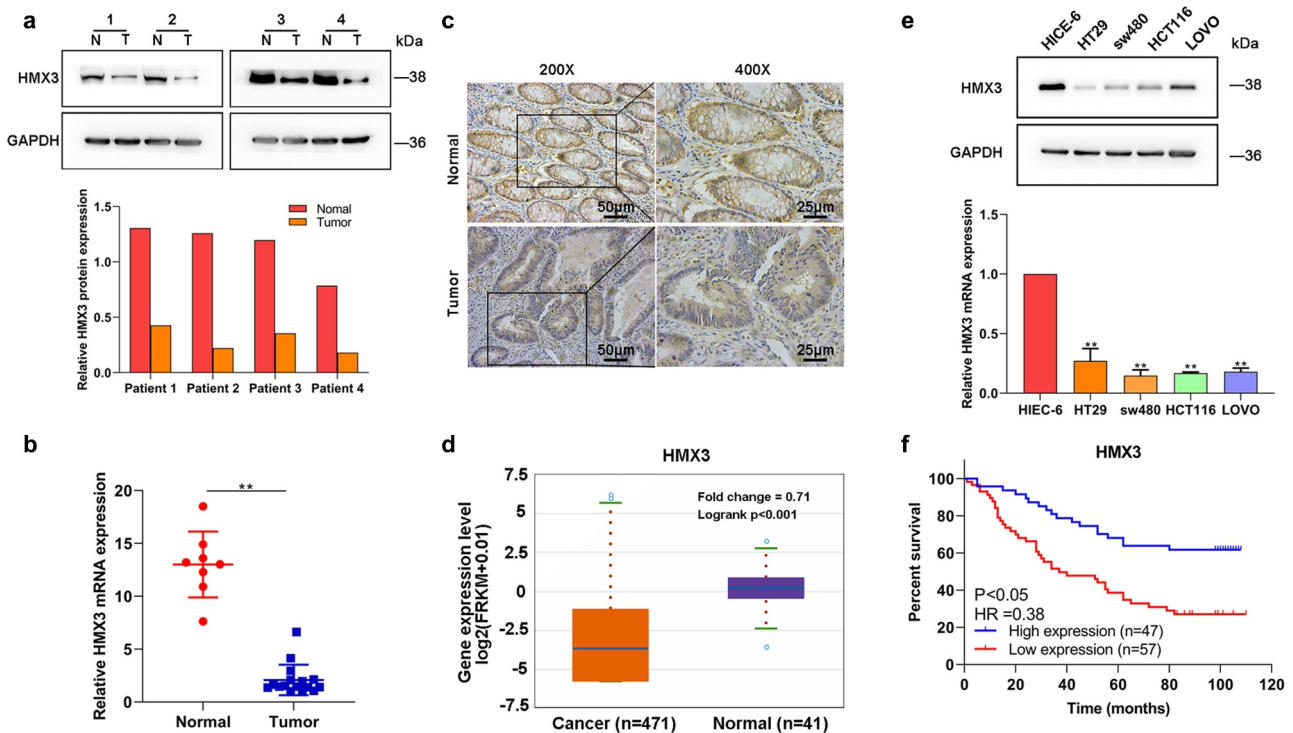


Figure 1. HMX3 was lowly expressed in CRC tissues (a) HMX3 protein expression and (b) mRNA expression in CRC tissues and adjacent normal tissues were measured by WB and qRT-PCR, respectively. (c) The representative IHC image for HMX3 expression pattern of CRC tissues and adjacent normal tissues (d) The HMX3 mRNA expression analysis between normal ($n = 41$) and CRC ($n = 471$) tissues from the ENCORI database. (e) The expression levels of HMX3 in normal human intestinal epithelial cells (HIEC-6) and CRC cell lines (HT29, HCT116, SW480 and LOVO) detected by WB (top) and qRT-PCR (bottom). (f) The overall survival analysis of CRC patients based on HMX3 expression ($n = 104$). $**P < 0.01$. All data represent mean \pm SD from at least three independent sets of experiment.

and protein levels in HCT116 and SW480 cells (Figure 2a). EdU assay illustrated that HMX3 overexpression resulted in an obvious decrease in counts of EdU incorporated cells compared with that in the vector group ($P < 0.05$, Figure 2b), suggesting a potent suppressive effect of HMX3 on CRC cell proliferation. The results of CCK-8 and colony formation assays were consistent with those of EdU assay ($P < 0.01$, Figure 2c and 2d), confirming that HMX3 overexpression could significantly inhibit CRC cell proliferation. To further corroborate the function of HMX3 on the cell proliferation of CRC, HMX3 expression was subsequently knocked down in HCT116 and SW480 cells by transfecting with shRNAs targeting HMX3 (sh-HMX3) and the negative control plasmids (NC) (Figure 2e). As expected, silencing HMX3 could significantly increase the proliferation rate of CRC cells when compared with the NC group, as demonstrated by EdU staining ($P < 0.005$, figure 2f), CCK-8 ($P < 0.005$, Figure 2g), and colony

formation assays ($P < 0.005$, Figure 2h). Notably, *in vivo* analysis also confirmed the above finding. The results showed that tumors formed by HMX3 overexpressed cells were much smaller than those formed by the control cells (Figure 2i). Additionally, the tumor growth in mice with HMX3 overexpression was slower than that in the control mice (Figure 2j). Taken together, these results indicated that HMX3 could remarkably suppress CRC cell proliferation *in vitro* and tumor growth *in vivo*.

HMX3 inhibits CRC cell migration and invasion

As acknowledged, the enhancement of migration and invasion is another characteristic of CRC progression, we further explored the effect of HMX3 on CRC cell migration and invasion. The Transwell assay showed that the number of invasive CRC cells in the HMX3 group was significantly lower (approximately 3-folds) than that in

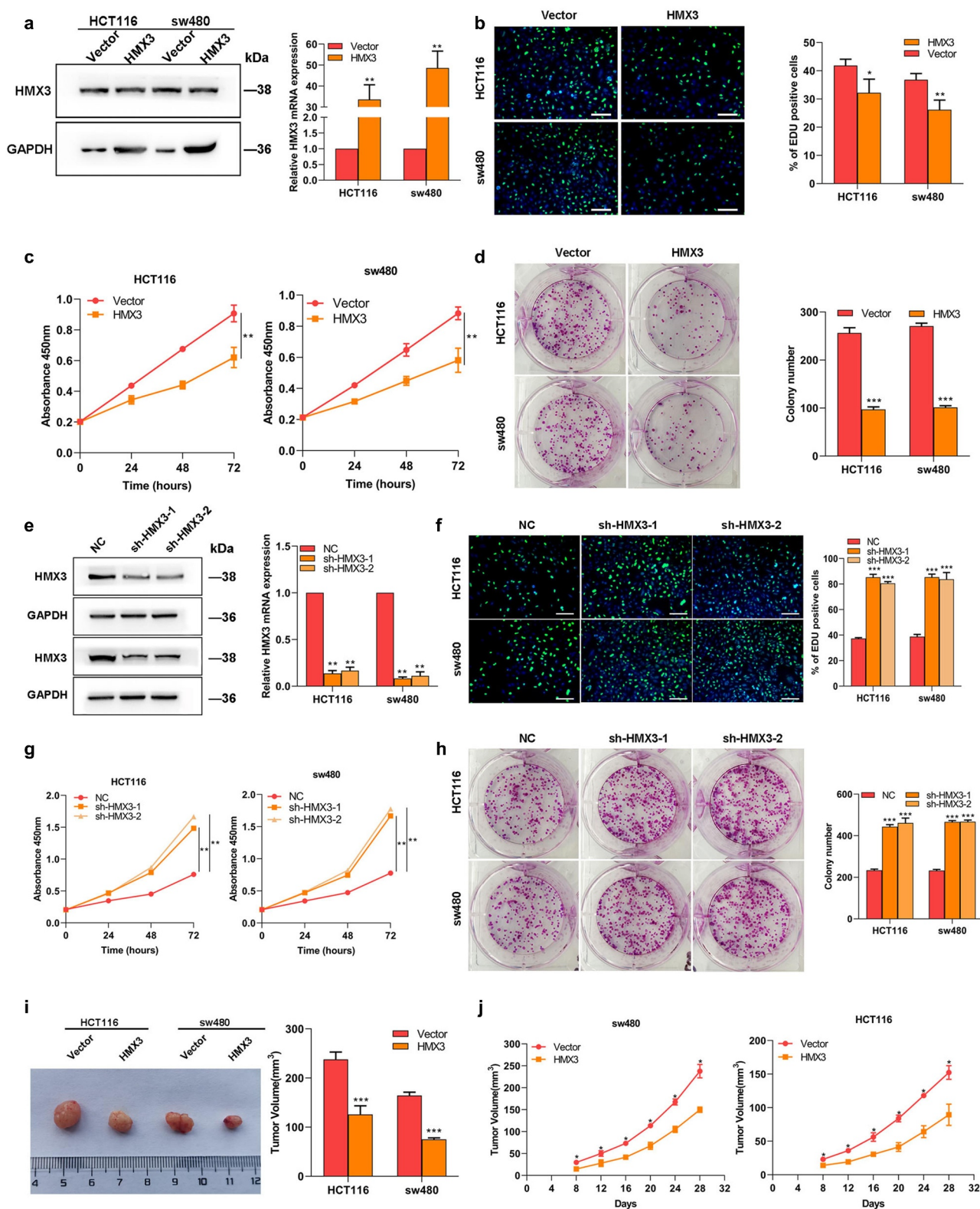


Figure 2. HMX3 suppresses CRC cell proliferation and tumor growth (a) The transfection efficiency detected by WB (top) and qRT-PCR (bottom) after HCT116 and SW480 cells were transfected with HMX3 overexpression plasmids (HMX3) or the control plasmids (Vector). The cell proliferation of HCT116 and SW480 cells assessed by (b) EdU staining, (c) CCK-8, and (d) colony formation assays following the transfection of HMX3 or Vectors. (e) The efficiency of HMX3 knockdown detected by WB (top) and qRT-PCR (bottom) after HCT116 and SW480 cells were transfected with short hairpin RNA-against HMX3 (sh-HMX3-1, sh-HMX3-2) or the negative control (NC). The cell proliferation of HCT116 and SW480 cells assessed by (f) EdU staining, (g) CCK-8, and (h) colony formation assays following the transfection of sh-HMX3-1, sh-HMX3-2, or NC. HCT116 and SW480 cells transfected with HMX3 or Vector were subcutaneously injected into nude mice, and xenografts were collected after 4 weeks. (i) The representative image (top) and volume (bottom) of xenografts. (j) Growth curve of xenografts. ** $P < 0.01$ and *** $P < 0.005$. All data represent mean \pm SD from at least three independent sets of experiment.

the vector group ($P < 0.005$, Figure 3a and 3B), indicating a suppression role of HMX3 in CRC cell invasion. Besides, the wound scratch assay also demonstrated that HXM3 could impair the migratory ability of CRC cells, as the overexpression of HMX3 noticeably decreased the migration distance of HCT116 and SW480 cells compared with the vector group ($P < 0.01$, Figure 3c and 3d). Conversely, the cell migration and invasion were significantly enhanced by the knockdown of HMX3 in HCT116 and SW480 cells (Figure 3e-h).

Epithelial-mesenchymal transition (EMT) is a process in which epithelial cells acquire mesenchymal features. It's widely accepted that EMT is associated with tumor initiation, invasion, and metastasis in cancer [21]. Surprisingly, our data showed that HMX3 overexpression led to a significant alteration in the expression levels of EMT-related proteins (E-cadherin, Vimentin, N-cadherin, MMP2, and MMP9) compared with the vector group (Figure 3i), suggesting that HMX3 may be a regulator in the EMT process. In summary, these findings indicated that HMX3 could suppress the migration and invasion of CRC cells, and inhibit the EMT process, which further verified the suppressive role of HMX3 in malignant behaviors of CRC cells.

In addition, we also preliminarily explored the mechanism behind the role of HMX3 in CRC progression by using GSEA tool and WB analysis (Figure S1). GSEA revealed that HMX3 expression was highly correlated with apoptosis (Figure S1A) and KRAS (Kirsten rat sarcoma viral oncogene homolog) signaling (Fig. S1B) pathways. Notably, the detection of apoptosis and KRAS signaling related protein levels verified the result of GSEA, indicating that HMX3 overexpression enhanced the expression levels of proapoptotic proteins (C-Caspase-9, C-Caspase-3, and Bax), suppressed the expression levels of antiapoptotic protein Bcl-2 (Fig. S1C), and also inactivated the PI3K/Akt/mTOR and MEK/ERK signaling pathways (Fig. S1D). Taken together, our results suggested the potential of HMX3 in regulating apoptosis and KRAS signaling pathways.

HMX3 is deubiquitinated by USP38 in CRC

To reveal the underlying mechanism of HMX3 in regulating CRC cell progression, the gene which

may interact with HMX3 was predicted using the BioGRID and GeneMANIA databases. The interaction networks for HMX3 are displayed in Figure 4a. Noticeably, there were two common genes in interaction networks, which were USP38 and STAMBPL1. Given that USP38 has been reported to suppress chemoresistance and stemness of CRC cells via deubiquitylating its target protein [18], we wonder whether USP38 participated in the role of HMX3 in CRC progression. Hence, USP38 was selected for further analyses.

The expression level of USP38 in CRC and corresponding adjacent normal tissues was determined using WB. The results showed that the protein expression level of USP38 in CRC tissues was considerably lower than that in adjacent normal tissues (Figure 4b). Consistent with this result, the analysis based on ENCORI confirmed that USP38 was lowly expressed in CRC tissues (Figure 4c). Next, Co-IP assay demonstrated that FLAG-tagged USP38 could strongly co-precipitate with HA-tagged HMX3 (Figure 4d), suggesting the interaction of USP38 and HXM3. Interestingly, it was found that there was a positive correlation between the expression levels of HMX3 and USP38 amounts (Figure 4e), which indicated that the expression of USP38 increased the stability of HMX3 protein to some extent. Moreover, an *in vitro* ubiquitination assay validated that the ubiquitination level of HMX3 was significantly decreased by USP38 overexpression (figure 4f), thereby protecting the HMX3 protein from degradation. To investigate the role of USP38 in protein levels through post-translational modifications, 10 mM CHX was used to determine the half-life of HMX3 proteins. USP38 knockdown could strikingly shorten the half-life of HMX3 protein in HCT116 cells (Figure 4g), whereas it was prolonged by USP38 overexpression (Figure 4h), implying that the USP38 could strengthen the protein stabilization of HMX3. Taken together, these data demonstrated that USP38 protects the HMX3 protein from degradation via deubiquitination to enhance its stabilization.

USP38 suppresses CRC cell proliferation, migration, and invasion through HMX3

To investigate whether USP38 regulates CRC cell progression in a HMX3-dependent manner, HCT116 and SW480 cells were transfected with

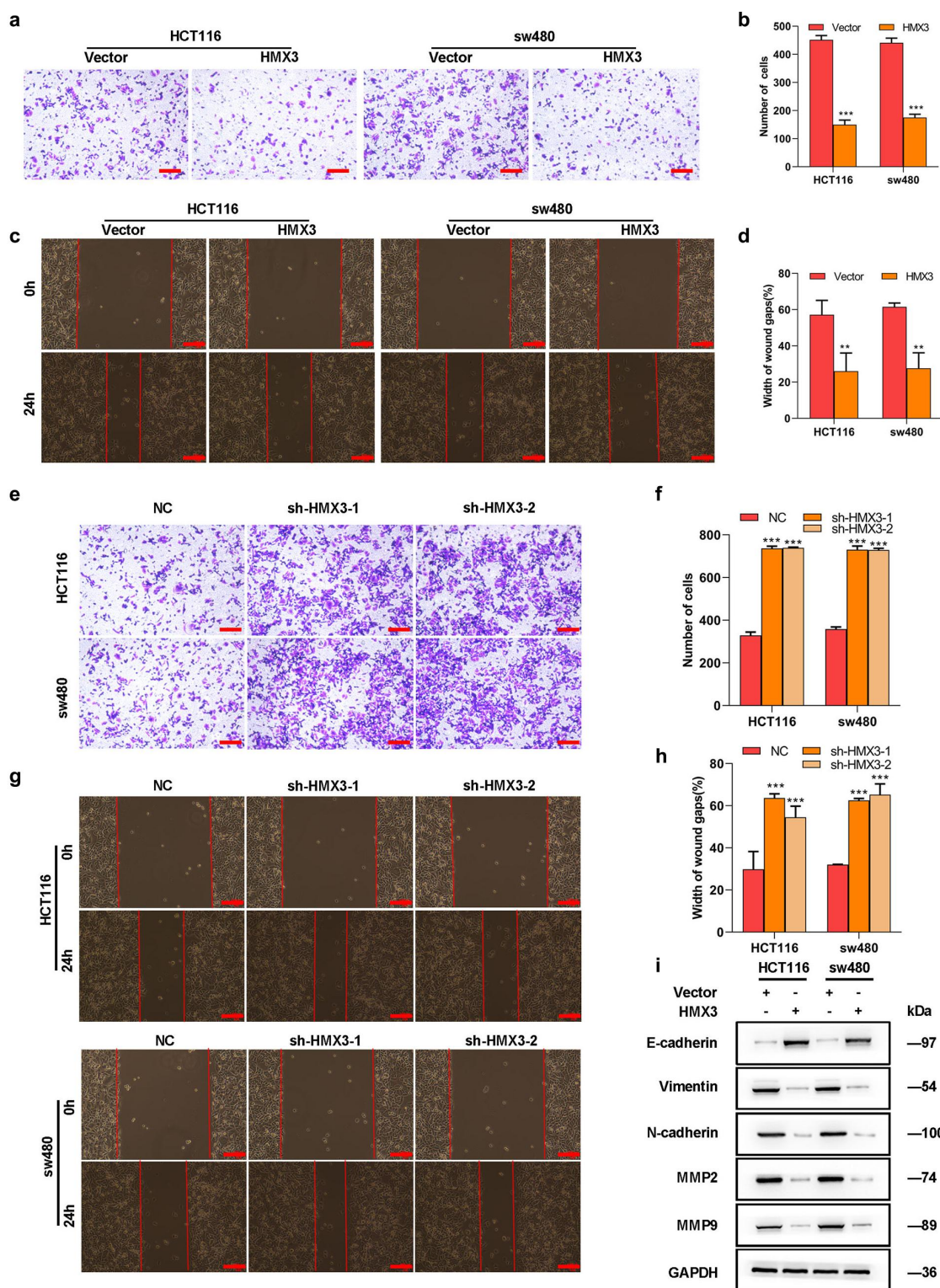


Figure 3. HMX3 suppresses CRC cell migration and invasion The invasive capacity of CRC cells transfected with HMX3 or Vectors evaluated by (a) Transwell assay and (b) the corresponding quantification analysis. The migration of CRC cells transfected with HMX3 and Vectors measured by (c) wound scratch assay and (d) the corresponding quantification analysis. The invasive capacity of CRC cells transfected with sh-HMX3-1, sh-HMX3-2, or NC detected by (e) Transwell assay and (f) the corresponding quantification analysis. The migration of CRC cells transfected with sh-HMX3-1, sh-HMX3-2, or NC measured by (g) wound scratch assay and (h) the corresponding quantification analysis. (i) The protein levels of E-cadherin, Vimentin, N-cadherin, MMP2 and MMP9 in CRC cells measured by WB following the transfection of HMX3 or Vectors. $**P < 0.01$. All data represent mean \pm SD from at least three independent sets of experiment.

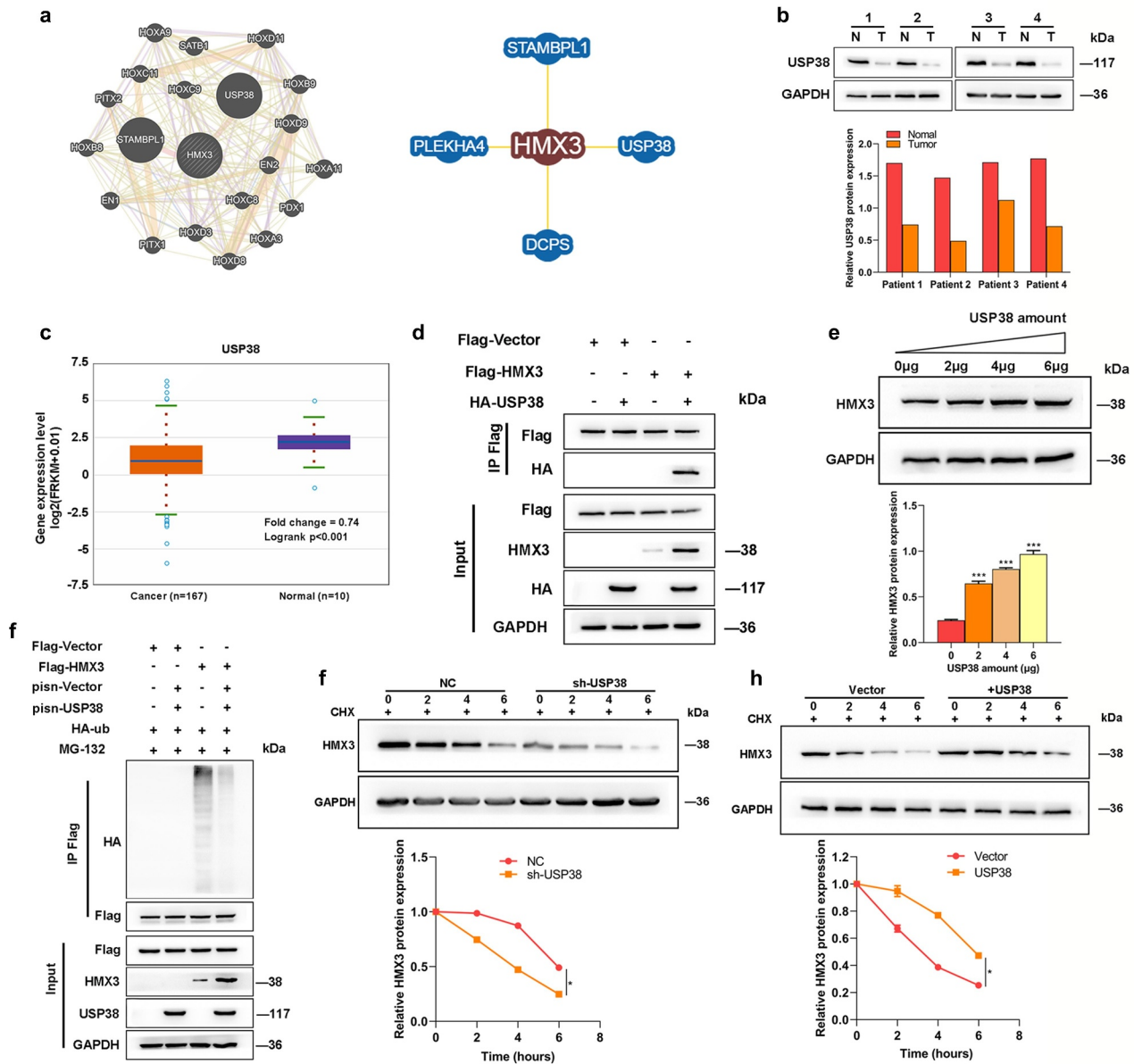


Figure 4. USP38 stabilizes HMX3 by deubiquitylation (a) The potential intersected genes of HMX3 predicted by BioGRID and GeneMANIA databases. (b) USP38 protein expression in CRC and the adjacent normal tissues from four patients measured by WB. (c) The USP38 mRNA expression analysis between normal ($n = 10$) and CRC ($n = 167$) tissues from the ENCORI database. (d) The interaction between HMX3 and USP38 verified by Co-IP assay; Flag-HMX3 and HA-USP38 expression plasmids were co-transfected into HEK293T cells, and the interaction between HMX3 and USP38 was determined by immunoprecipitation with α -Flag beads followed by immunoblotting with α -HA or α -Flag antibody. (e) Increasing amounts of USP38 were transfected into HCT116 cells and HMX3 expression was detected by WB. (f) Flag-HMX3, pisn-USP38, and HA-Ub expression plasmids were co-transfected into HEK293T for 48 h. After the cells were treated with 10 mM MG132 for 6 h, HMX3 was immunoprecipitated with anti-Flag agarose beads, and the ubiquitination of HMX3 was examined by WB using anti-HA antibody. After treating with 50 mg/mL CHX for 0, 2, 4 and 6 h, the HMX3 expression levels in (g) USP38 silencing HCT116 cells and (h) USP38 overexpressing HCT116 cells were examined by WB. * $P < 0.05$ and *** $P < 0.005$. All data represent mean \pm SD from at least three independent sets of experiment.

USP38 shRNA plasmids (sh-USP38) alone or co-transfected with HMX3 overexpression plasmids. After USP38 was knocked down in CRC cells, the EdU incorporated cells were significantly

increased; however, this increase was blocked by HMX3 overexpression ($P < 0.005$, Figure 5a). CCK-8 and colony formation assays also showed the suppressive role of sh-USP38 in the

proliferation of CRC cells was blocked by HMX3 overexpression ($P < 0.01$, Figure 5b and 5c). Concerning CRC cell migration and invasion, it was observed that USP38 silencing facilitated the migratory and invasive abilities of CRC cells, which could be restrained by HMX3 overexpression ($P < 0.05$, Figure 5d and 5e). It was found that silencing USP38 in HCT116 cells led to an obvious decrease in HMX3 expression (Figure 5f). Moreover, the effect of USP38 knockdown on the expression levels of EMT-related proteins was also blocked by HMX3 overexpression (Figure 5f). Collectively, these findings demonstrated that USP38 suppressed CRC cell proliferation, migration, and invasion through HMX3.

Discussion

In this study, our results illustrated that HMX3 was lowly expressed in CRC tissues and cell lines. Lower HMX3 expression in CRC patients was associated with a poor prognosis. Additionally, HMX3 overexpression suppressed HCT116 and SW480 cell proliferation, migration, and invasion, while HMX3 silencing exerted the converse effect. Moreover, HMX3 overexpression also exerted a potential suppression effect on the EMT process in CRC cells and tumor growth *in vivo*. Although previous studies have mainly focused on the role of HMX3 in the nervous system, such as the inner ear and hypothalamus [5,22], the findings in this study implied that HMX3

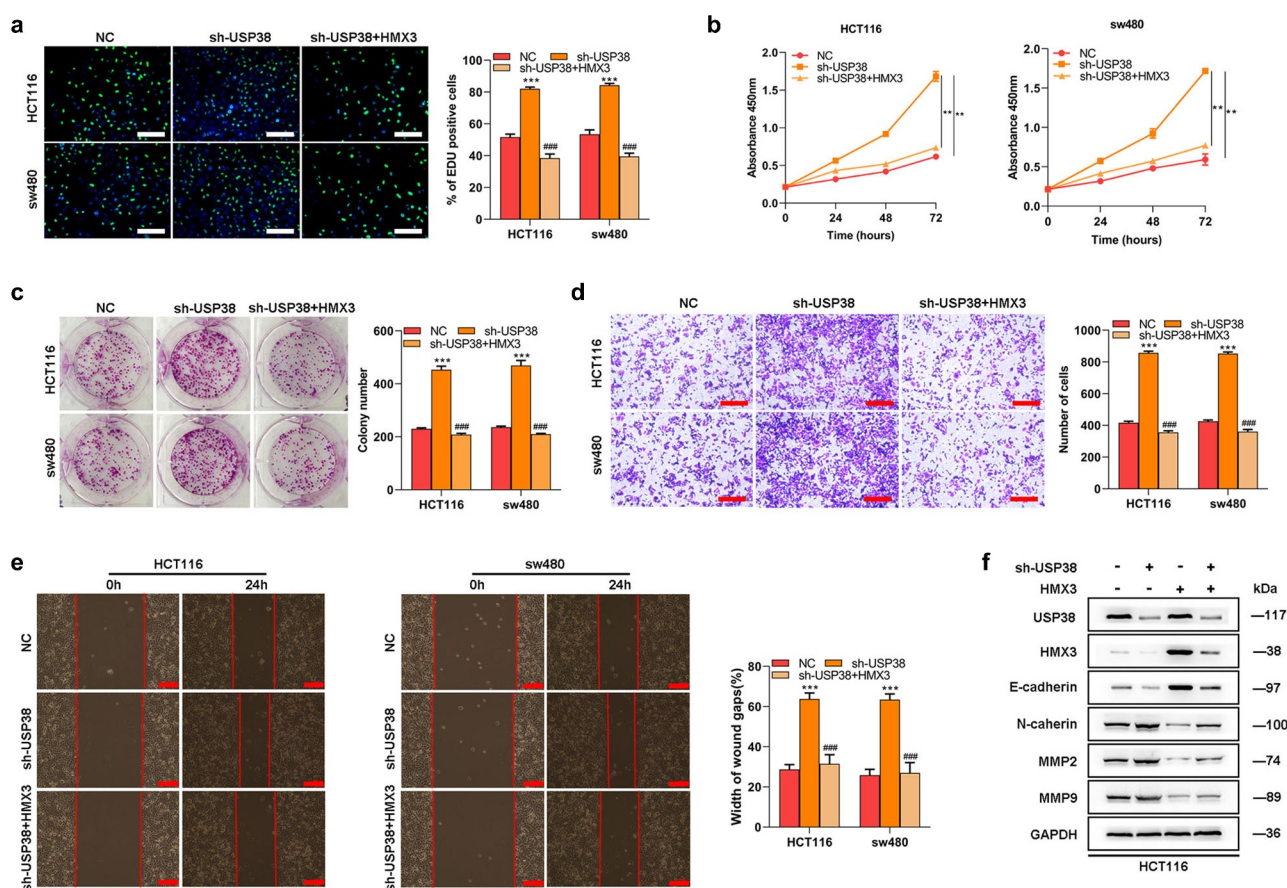


Figure 5. USP38 suppresses CRC cell proliferation, migration and invasion through HMX3 HCT116 and SW480 cells were transfected with short hairpin RNA-against USP38 (sh-USP38) or the negative control (NC) or the combination of sh-USP38 with HMX3 overexpression vectors (HMX3). Cell proliferation determined by (a) EdU staining, (b) CCK-8, and (c) colony formation. (d) Cell invasion measured by Transwell assay. (e) Cell migration evaluated by wound scratch assay. (f) The protein levels of E-cadherin, Vimentin, N-cadherin, MMP2 and MMP9 measured by WB. ** $P < 0.01$ and *** $P < 0.005$; ### $P < 0.005$, versus the sh-USP38 group. All data represent mean \pm SD from at least three independent sets of experiment.

might be a tumor suppressor in the development and progression of CRC.

Next, a bioinformatics tool-GSEA was used to primitively explore the potential pathways related to the role of HMX3 in CRC development and progression. Our data suggested significant associations between HMX3 expression and apoptosis and KRAS signaling. The induction of apoptosis is recognized as an important acting mechanism of a tumor suppressor gene [23]. Our further WB analysis confirmed the result of GSEA, indicating that HMX3 overexpression could up-regulate c-caspase-9, c-caspase-3, and Bax proteins levels in both HCT116 and SW480 cells, indicating that HMX3 might also act on the malignant phenotype of CRC cells by inducing apoptosis. KRAS, a small guanosine triphosphate (GTP) binding protein, is one of front-line sensors that initiate the activation of various signaling pathways, including PI3K and MAPK pathways [24]. Recently, a study showed that silencing KRAS repressed the activation of PI3K/Akt/mTOR signaling pathway, thereby regulating the EMT of breast cancer cells [25]. Consistently, our study showed HMX3 overexpression caused not only a down-regulation of KRAS but also an inactivation of PI3K/Akt/mTOR and MEK/ERK signal pathways in CRC cells; and our previous data also showed HMX3 overexpression could block the EMT of CRC cells. Notably, our studies showed the effect of HMX3 on the expression level of Bcl-2 and p-mTOR was different between HCT116 and SW480 cells. It is speculated that this is because the HCT116 cell line has the microsatellite instability phenotype while the SW480 cell line does not [26]. However, there are few studies on the regulatory role of HMX3 in apoptosis and KRAS signaling, and the precise mechanism could be a promising clue for future studies on the role of HMX3 in CRC.

To explore the possible regulatory mechanism through which HMX3 suppressed the proliferation, migration, and invasion of CRC cells, we applied the online bioinformatics databases of BioGRID and GeneMANIA and predicted USP38 as a potential interacted gene of HMX3. Given that USP38 is a member of DUBs that maintain the high level of their targeted protein by overriding the ubiquitination-mediated degradation process, we speculated that the down-regulation of HMX3 in CRC is the

result of the deubiquitination modification by USP38. The WB analysis on clinical samples and bioinformatics analysis on ENCORI online database revealed that USP38 is lowly expressed in CRC. In addition, the functional results revealed that genetic deletion of USP38 promoted cell proliferation, migration, invasion, and EMT process in CRC *in vitro*, supporting that USP38 might be a tumor suppressor in CRC. Armakolas et al. revealed a significant association between patients with HER2 subtype breast cancer and USP38 expression [27]. It has been reported that USP38 serves as a tumor suppressor in kidney renal clear cell carcinoma by regulating cancer cell response to genotoxic insults [28]. Zhan et al. demonstrated USP38 contributes to the stemness and chemoresistance of CRC cells via its function of deubiquitination on HDAC3 [18]. Similarly, in this study, USP38 was proven to directly interact with HMX3 and stabilize its protein level via deubiquitination. Biologically, HMX3 overexpression reversed the suppressive effects on malignant behaviors of CRC cells induced by USP38 silencing. Notably, our data also showed there was no change in the USP38 expression levels of CRC cells after transfecting with HMX3 overexpression. These results collectively supported that HMX3 is an essential substrate for USP38-mediated cell proliferation, migration, and invasion.

In conclusion, our study demonstrated that HMX3 is lowly expressed in CRC, and HMX3 expression was negatively correlated with poor prognosis of CRC patients. USP38 could impede the protein degradation of HMX3 through deubiquitination to suppress the proliferation, migration, and invasion of CRC cells. Hence, triggering HMX3/USP38 axis may be a potent therapeutic strategy against CRC. However, the precise mechanism behind the suppression role of HMX3/USP38 axis in CRC progression still remains to be explored.

Acknowledgments

None.

Disclosure statement

No potential conflict of interest was reported by the author(s).

Funding

Departmental Sources.

Data availability statement

The data used to support the findings of this study are available from the corresponding author upon request.

References

- [1] Sung H, Ferlay J, Siegel RL, et al. Global cancer statistics 2020: GLOBOCAN estimates of incidence and mortality worldwide for 36 Cancers in 185 Countries. *CA Cancer J Clin.* **2021**;71(3):209–249.
- [2] Feng M, Zhao Z, Yang M, et al. T-cell-based immunotherapy in colorectal cancer. *Cancer Lett.* **2021**;498:201–209.
- [3] Roknic N, Huber A, Hegemann SCA, et al. Mutation analysis of Netrin 1 and HMX3 genes in patients with superior semicircular canal dehiscence syndrome. *Acta Otolaryngol.* **2012**;132(10):1061–1065.
- [4] Ohta S, Wang B, Mansour SL, et al. BMP regulates regional gene expression in the dorsal otocyst through canonical and non-canonical intracellular pathways. *Development.* **2016**;143(12):2228–2237.
- [5] Wang W, Grimmer JF, Van De Water TR, et al. Hmx2 and Hmx3 homeobox genes direct development of the murine inner ear and hypothalamus and can be functionally replaced by *Drosophila* Hmx. *Dev Cell.* **2004**;7(3):439–453.
- [6] Wang W, M Frasch P Lo, Lufkin T. Hmx: an evolutionary conserved homeobox gene family expressed in the developing nervous system in mice and *Drosophila*. *Mech Dev.* **2000**;99(1–2):123–137.
- [7] Fuentes-Antrás J, Alcaraz-Sanabria AL, Morafraila EC, et al. Mapping of genomic vulnerabilities in the post-translational ubiquitination, SUMOylation and neddylation machinery in breast cancer. *Cancers (Basel).* **2021**;13(4):833.
- [8] Scheffner M, Nuber U, Huibregtse JM. Protein ubiquitination involving an E1-E2-E3 enzyme ubiquitin thioester cascade. *Nature.* **1995**;373(6509):81–83.
- [9] Isaacson MK, Ploegh HL. Ubiquitination, ubiquitin-like modifiers, and deubiquitination in viral infection. *Cell Host Microbe.* **2009**;5(6):559–570.
- [10] Li Y, Shi F, Hu J, et al. The role of deubiquitinases in oncovirus and host interactions. *J Oncol.* **2019**;2019:2128410.
- [11] Sahtoe DD, Sixma TK. Layers of DUB regulation. *Trends Biochem Sci.* **2015**;40(8):456–467.
- [12] Li Y, Shi F, Hu J, et al. Stabilization of p18 by deubiquitylase CYLD is pivotal for cell cycle progression and viral replication. *NPJ Precis Oncol.* **2021**;5(1):14.
- [13] Cruz L, Soares P, Correia M. Ubiquitin-specific proteases: players in cancer cellular processes. *Pharmaceuticals (Basel).* **2021**;14(9):848.
- [14] Wu Y, Zhang Y, Wang D, et al. USP29 enhances chemotherapy-induced stemness in non-small cell lung cancer via stabilizing Snail1 in response to oxidative stress. *Cell Death Dis.* **2020**;11(9):796.
- [15] Shin S, Kim K, Kim H-R, et al. Deubiquitylation and stabilization of Notch1 intracellular domain by ubiquitin-specific protease 8 enhance tumorigenesis in breast cancer. *Cell Death Differ.* **2020**;27(4):1341–1354.
- [16] Lin M, Zhao Z, Yang Z, et al. USP38 inhibits type I interferon signaling by editing TBK1 ubiquitination through NLRP4 signalosome. *Mol Cell.* **2016**;64(2):267–281.
- [17] Zhao Z, Su Z, Liang P, et al. USP38 couples histone ubiquitination and methylation via KDM5B to resolve inflammation. *Adv Sci (Weinheim, Baden-Wuerttemberg, Germany).* **2020**;7(22):2002680.
- [18] Zhan W, Liao X, Liu J, et al. USP38 regulates the stemness and chemoresistance of human colorectal cancer via regulation of HDAC3. *Oncogenesis.* **2020**;9(5):48.
- [19] Franken NA, Rodermond HM, Stap J, et al. Clonogenic assay of cells in vitro. *Nat Protoc.* **2006**;1(5):2315–2319.
- [20] Brix N, Samaga D, Belka C, et al. Analysis of clonogenic growth in vitro. *Nat Protoc.* **2021**;16(11):4963–4991.
- [21] Pastushenko I, Blanpain C. EMT transition states during tumor progression and metastasis. *Trends Cell Biol.* **2019**;29(3):212–226.
- [22] Feng Y, Xu Q. Pivotal role of hmx2 and hmx3 in zebrafish inner ear and lateral line development. *Dev Biol.* **2010**;339(2):507–518.
- [23] Farnebo M, Bykov VJ, Wiman KG. The p53 tumor suppressor: a master regulator of diverse cellular processes and therapeutic target in cancer. *Biochem Biophys Res Commun.* **2010**;396(1):85–89.
- [24] Liu P, Wang Y, Li X. Targeting the untargetable KRAS in cancer therapy. *Acta Pharm Sin B.* **2019**;9(5):871–879.
- [25] Zhang Y, Liu JL, Wang J. KRAS gene silencing inhibits the activation of PI3K-Akt-mTOR signaling pathway to regulate breast cancer cell epithelial-mesenchymal transition, proliferation and apoptosis. *Eur Rev Med Pharmacol Sci.* **2020**;24(6):3085–3096.
- [26] Michael-Robinson JM, Biemer-Hüttmann A, Purdie DM, et al. Tumour infiltrating lymphocytes and apoptosis are independent features in colorectal cancer stratified according to microsatellite instability status. *Gut.* **2001**;48(3):360–366.
- [27] Armakolas A, Stathopoulos GP, Nezos A, et al. Subdivision of molecularly-classified groups by new gene signatures in breast cancer patients. *Oncol Rep.* **2012**;28(6):2255–2263.
- [28] Yang Y, Yang C, Li T, et al. The deubiquitinase USP38 Promotes NHEJ repair through regulation of HDAC1 activity and regulates cancer cell response to genotoxic insults. *Cancer Res.* **2020**;80(4):719–731.